Hindawi
International Transactions on Electrical Energy Systems
Volume 2022, Article ID 7584424, 13 pages
https://doi.org/10.1155/2022/7584424

Research Article

A Multi-Agent Optimal Bidding Strategy in Multi-Operator VPPs Based on SGHSA

Shupeng Li,[1] Xianxu Huo,[1] Xiyuan Zhang,[2] Guodong Li,[1] Xiangyu Kong,[2] and Siqiong Zhang[2]

[1]*Tianjin Electric Power Company Electric Power Science Research Institute, Tianjin 300384, China*
[2]*Key Laboratory of Smart Grid of Ministry of Education, Tianjin University, Tianjin 300072, China*

Correspondence should be addressed to Xianxu Huo; huoxianxu@gmail.com and Xiyuan Zhang; zhangxiyuanr@tju.edu.cn

Received 4 June 2022; Revised 28 July 2022; Accepted 5 October 2022; Published 20 October 2022

Academic Editor: Ci Wei Gao

As an individual plant participating in the power market, the virtual power plant (VPP) is regarded as the ultimate configuration of the energy Internet, and effective dispatching is a challenge. This paper proposes a multi-agent optimal bidding strategy based on a self-adaptive global optimal harmony search algorithm (SGHSA) to solve the problem of multi-operator participation in virtual power station scheduling. The method takes multiple agents to simulate the bidding process in the VPPs and distributes the profits for the operators based on the market mechanism to optimize the distributed energy resources (DERs). Case studies are provided and show that the proposed method realizes the optimal distribution of power generation and demand level, which improves the comprehensive advantage of the VPP in electricity market transactions.

1. Introduction

A virtual power plant (VPP) is a necessary form of the future energy Internet, which participates in the power market as an individual power unit [1]. Based on the advanced information and communication technology, the VPP integrates distributed energy resources (DERs) such as distributed power generation (DG), energy storage, controllable load, and electric vehicles to coordinate and optimize them to achieve the stability and reliability of their overall output to the main grid [2]. Under the current model, the electricity price of the virtual power plant is the same as the power supply's price of the main grid to which the VPP is connected. However, the power supply's price of the main grid fluctuates from peak to valley level due to the supply-demand relationship and other factors, which cannot motivate the enthusiasm of the virtual power plant to implement a load shift of the power grid [3]. Therefore, determining the purchase price of the VPP needs to consider multiple factors.

A virtual power plant imitates the function of a traditional large power plant by centralized scheduling and intelligent control of the DERs [4]. The internal and external interaction units involved in the virtual power plant are shown in Figure 1. The VPP realizes the overall coordinated regulation of distributed energy resources, energy storage, and various loads through advanced data communication and coordinated control technology and interacts with power grid companies and power distribution companies to participate in the demand-side management and power grid auxiliary services.

When it comes to the interaction between the VPP and the power grid and the optimal internal scheduling of the VPP, the VPP is generally thought of as a management system representing the DERs in transactions with the grid. The DER output is arranged by the maximum overall benefit or the minimum operating cost of the VPP. In this mode, each DER is owned by the VPP by default, and the corresponding compensation is given to the controllable load in the VPP. The VPP has absolute power control over the output of the DER; that is, there is just one DER operator in a VPP [5]. With the large-scale development of the DERs, the investment subject of the DERs gradually showed a trend of diversification, and the DERs in the VPP may be owned by different operators [6].

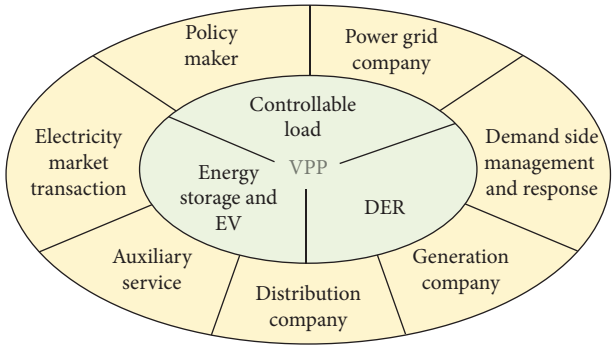

Figure 1: The internal and external interaction units involved in the VPP.

Meanwhile, there are several operators in a VPP, and each operator has different interest demands. Suppose we ignore the self-interests of each operator in the VPP and only focus on the overall benefits of the VPP. In that case, the DER operators and load aggregators will lack the enthusiasm to join the virtual power plant, which hinders the promotion and development of the virtual power plant [7]. Therefore, how to take into account the interest demands of each operator, how to make a reasonable scheduling plan, and how to improve the enthusiasm of multiple operators are the challenges for the VPP dispatching center.

Generally, there are two kinds of transaction modes and benefit distribution mechanisms for the distributed energy participating in the market: the price changes over time and the bidding pattern. Under the price changes pattern over time, operators of the DERs schedule their power generation based on the VPP's internal real-time electricity price, which includes particular interest game behavior. In [8], a VPP scheduling model including photovoltaic, wind power, hydropower, and other energy sources was established, which realized the coordinated operation of various DERs, but it did not involve the benefit distribution of each operator. In [9], a microgrid optimization method based on multi-agent bidding equilibrium was proposed to distribute the benefits to the investors of the DERs, but the uncertainty of the renewable energy generation is not considered. In [10], an optimal economic dispatch of virtual power plant based on bidding is proposed to achieve optimal power generation of distributed generation in VPPs. In [11], a bi-level multi-time scale scheduling method based on bidding for multi-operator VPP was proposed to provide a framework for solving profit allocation and optimal scheduling problems. However, this paper did not describe how the operators determine their bidding function.

Under the bidding mode, the DERs inside the VPP offer their prices and quantities to the market, and if their bid price is accepted, they will sell their power at the winning price. The bidding strategy of the DERs is crucial in the bidding mode; however, there are few pieces of research in this field, and most of them focus on the bidding strategy of the VPP participating in the electricity market. Kardakos et al. [12] studied the strategic bidding behavior of the VPP with distributed energy, storage systems, and power users participating in the day-ahead electricity market. Shafiekhani et al. [13] modeled the bidding behaviors of the VPP and generation companies and studied the bidding process of the VPP and other strategic competitors (generation companies) in the day-ahead electricity market. In [14], the bi-level equilibrium model was established to study the interaction in multiple energy sources when they participated in the electricity market, competing with the generation company in different ways and influencing the market equilibrium results. However, all the above studies regard the VPP as an internal aggregation without any conflict of interest to participate in the power market.

Like the research on virtual power plants, microgrids can also realize the function of aggregating distributed energy by connecting distributed energy to the grid. Ahmad et al. [15] proposed a joint energy management and trading model to provide low-cost power consumption for distribution systems. Ahmad et al. [16] offered a strategy integrating distributed energy, load scheduling, energy storage system, and feed to effectively utilize energy and develop an autonomous system that can manage all these resources effectively and efficiently. Ahmad et al. [17] put forward a uniform DSM model used to reduce the electricity costs and demand during the peak hours. The simulation results show that the model achieves excellent performance and can effectively reduce the carbon dioxide emissions. Still, the study did not consider the consumer's privacy. The implementation complexity of the proposed model is also high. In [18], a single management system was formed by considering the consumer's preference, priority, ease of use, power grid stability, minimum deviation, smoothness of demand curve, and the insertion cost. The system will also provide consumers' privacy as it would mask the energy usage pattern that combines psychological incentives in addition to economic benefits. It will also protect the consumer's privacy. In [19], the concept of domain and constraint reduction was applied to reduce the number of variables and the number of constraints of the given REM mathematical model in residential areas, simplifying the complexity of the mathematical model.

Self-adaptive global optimal harmony search algorithm (SGHSA) is an improvement of the traditional harmony search algorithm (HS) by Mojtaba et al., which can ensure global optimization and rapid convergence [20]. The algorithm simulates the process by which musicians repeatedly adjust the pitch of each instrument in the band according to their memory to achieve an excellent harmonic state [21,22]. In SGHSA, the solution vector is called "harmony." If an optimization problem has k decision variables, a harmony vector is k-dimensional. The initial harmony vector group is generated randomly and stored in the harmony memory (HM). The optimization process consists of the initialization of the HM, the improvisation of the new harmony, and the update of the HM. The pros and cons of the created harmony vector are judged by the objective function [23].

The harmony memory considering rate (HMCR) is the probability of choosing a harmony from HM. Substantial HMCR value is conducive to local search, while small HMCR value enriches the diversity of the harmony library. The pitch adjusting rate (PAR) is the adjustment rate of the

selected x_{best}. A substantial PAR value is helpful to transfer x_{best}' information to the next generation, thus improving the local search capability performance around x_{best}, while a small PAR value can increase the diversity of the HM [24]. Because the local application and global exploration are always contradictory in the search process, it is not easy to identify the specific value of HMCR and PAR.

As the values of HMCR and PAR are not fixed in SGHSA, the HMCR (PAR) is assumed to follow a normal distribution. Through a certain number of iterations, the appropriate HMCR (PAR) value is found for later iteration solutions to adapt to specific problems and stages of the search, which gives attention to local and global search areas. Compared with ordinary HS, SGHSA has more advantages in solving problems due to its dynamic parameter adjustment. SGHSA is an intelligent algorithm with a simple concept, easy implementation, strong robustness, high efficiency, and fewer requirements [25] and has been widely applied in various fields, such as construction engineering [26], materials engineering [27], engineering design optimization [28], route planning [29], and medical field [30]. In addition, other algorithms have been proposed to deal with the bidding problems, and Zhang et al. [31] presented a new bidding strategy (BS) in which the wind power suppliers act as the price setters. The new algorithm, called the evolutionary game method (EGA), is inspired by the hybrid particle swarm optimization and the improved firefly algorithm (HPSOIFA). Compared with the conventional methods, the predictor can reduce the uncertainty of wind generation and BM price.

Regarding the internal energy optimal scheduling problem of the VPP, it is less engaged in the distribution of interests of numerous DER operators inside the VPP, and it is assumed that the VPP or a single operator owns the DERs, according to the above study materials. As a result, this research proposes a multi-agent optimum bidding method in multi-operator VPPs based on SGHSA. To accomplish optimization, the system uses the MAS control structure of the multi-operator VPP, sharing the earnings of various operators through the market mechanism. SGHSA is proposed to enable the DERs to get the optimal bidding function, which is then submitted to the bidding manager agent to optimize the owners' interests. The bidding manager agent creates a new internal electricity price based on the bidding function, which is then passed back to the DERs to enable them to develop the next round of strategies until the outcome reaches equilibrium. The following are the primary innovative contributions of the suggested technique.

(1) Considering the interest demands of each DER operator, to increase the excitement of the DER operators to participate in the VPP, the internal market trading mechanism is designed to offer a framework for handling the interest distribution among operators and optimum scheduling issues of the multi-operator VPP.

(2) Aiming at the shortcomings of the traditional harmony algorithms, such as slow convergence and low search accuracy, an improved adaptive global optimal harmony search algorithm (SGHSA) was proposed. SGHSA has the ability of dynamic learning to adapt to specific problems and stages of the bidding function search, maximizing the profits of the bidding agent.

(3) The proposed bidding strategy can obtain the bidding function through the bidding unit agent. After the internal price of the VPP is received, the uncertainty of the renewable energy generation is considered.

The remainder of the paper is structured as follows. Section 2 describes the MAS framework for multi-operator VPPs. Section 3 suggests the bidding and clearance procedure. Section 4 describes the flowchart for calculating the optimal bidding function using SGHSA. Section 5 presents case studies and analytic results. Section 6 draws the conclusion.

2. The MAS Framework of Multi-Operator VPP

The multi-operator virtual power plant means that different investment entities own the DERs within the VPP. The owner of the VPPs just signs contracts with the DER operators to allow the DERs to join the centralized dispatching power generation in the VPP, without mastering the technical details such as the generation cost of the DERs [32]. Wind turbines (WTs), photovoltaic cells (PV cells), micro-gas turbines (MTs), demand response (DR), battery storage, electric vehicles (EVs), and other resources are among the renewable energy sources used by the operators in this paper.

Because of MAS's intelligence, independence, and coordination, it can transform a global control problem into a distributed optimization problem of multi-level and multiple control systems, resulting in overall system economy and stability. In the last several years, it has been widely used in the energy management of microgrids and VPP [33], coordinated control [34], bidding operation [35], and other aspects. Therefore, based on the MAS structure adopted in [36], this paper constructs the layered structure virtual power plant operation architecture, as shown in Figure 2.

Top Layer. VPP dispatching center agent, as the top layer of a management unit in the VPP, can interact with the main grid on behalf of the VPP, such as the purchase and sale of electricity based on the price or contract.

Second Layer. This layer contains functional agents such as the bidding manager agent and operation control agent, which can manage the lower level of agents and accept the management of the upper level. The operation control agent shares the current operating condition of the VPP with the bid manager agent and receives scheduling optimization results of the power generation operation returned by the bidding manager agent. The bidding manager agent manages the bidding process in the VPP, obtains the economic distribution scheme of power generation, shares the scheme with the operation control agent, and reports the electricity price received from the bidding to the VPP dispatching center agent.

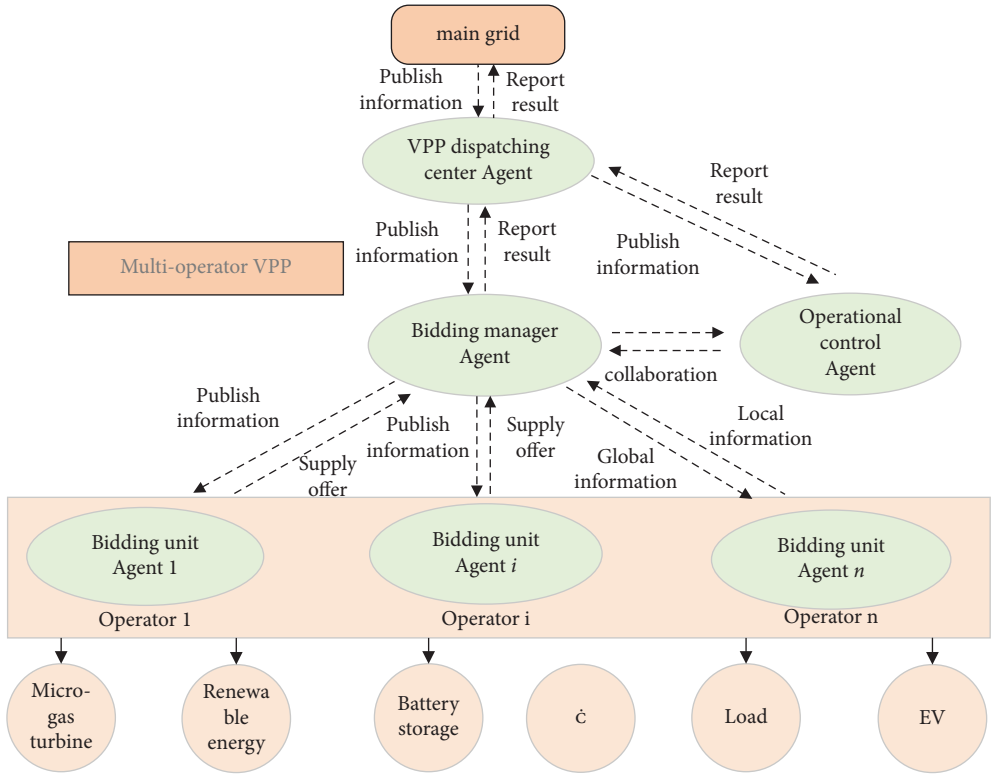

Figure 2: The internal bidding MAS framework of multi-operator VPP.

Third Layer. This layer involves the execution agents, such as the bidding unit agent, which accepts the management of the second layer agent. The bidding agent simulates the economic behavior of the rational person in economics, takes the maximization of their interests as the goal, and carries out bidding behavior under the management of the bidding management agent. The bidding unit agent makes bidding decisions based on local measurement information and communication information with other agents and submits the bidding strategy to the bidding manager agent.

3. Bidding and Clearing Process of Multi-Operator VPP

3.1. Optimal Bidding Strategy Model of Agents. If there are k operators in the VPP, there should be k bidding unit agents. Under the existing internal power pricing, each bidding unit agent tries to maximize its interests. In the bidding round n, the profit function of operator i is represented in the following equation:

$$\max F_i^n = P^n \times Q_i^n - C_i, \tag{1}$$

where F_i^n is the operator i's profit, P^n is the internal power price at the bidding round n, and Q_i^n is the operator i's reported electricity output.

As indicated in (2) [37], the cost of electricity generation assumes a quadratic function. C_i is the converted cost after taking into account the following components and environmental protection measures like clean energy subsidies and carbon trading, and C_i^1 and C_i^0 are convertible cost coefficients, while C_i^{const} is the fixed cost coefficient.

$$C_i = C_i^1 \left(Q_i^n\right)^2 + C_i^0 Q_i^n + C_i^{\text{const}}. \tag{2}$$

The operators have a variety of DER units, each with a different cost. As a result, the DER cost coefficient must be translated to obtain the operators' overall power-generating cost. The exact conversion formula may be seen below [11]. In the n$^{\text{th}}$ round of bidding, for the operator i,

$$C_i^{\text{const}} = \sum_{j \in E_i} c_{i,j}^{\text{const}}, \tag{3}$$

$$C_i^0 = c_i^{flu} \times \frac{\sum_{j \in E_i} c_{i,j}^0 Q_{i,j}^n}{Q_i^n}, \tag{4}$$

$$C_i^1 = c_i^{\text{flu}} \times \frac{\sum_{j \in E_i} c_{i,j}^1 \left(Q_{i,j}^n\right)^2}{\left(Q_{i,j}^n\right)^2}, \tag{5}$$

$$c_i^{\text{flu}} = 1 + \frac{\delta_{WT} \times \sum_{k \in E_i^{wt}} Q_{i,k}^n + \delta_{PV} \times \sum_{l \in E_i^{PV}} Q_{i,l}^n}{\sum_{k \in E_i^{wt}} Q_{i,k}^n + \sum_{l \in E_i^{PV}} Q_{i,l}^n}, \tag{6}$$

where c_i^{flu} is the operator i's fluctuating cost coefficient, j is the number of pieces of equipment that operator i owns, and integers l and k represent the number of PVs and WTs, respectively. The convertible cost coefficients of the equipment j are $c_{i,j}^1$ and $c_{i,j}^0$. The electricity output of the device j is denoted by $Q_{i,j}^n$; $c_{i,j}^{\text{const}}$ is the equipment j's fixed cost coefficient; E_i is the sum of all devices that participated in the

bidding procedure; and δ_{WT} and δ_{PV} represent the mean error coefficients of WT and PV power generation forecast, respectively. In the auction procedure, E_i^{WT} and E_i^{PV} are the total number of WTs and PVs that participated in the bidding. The output of the WT k and the PV l is referred to as $Q_{i,k}^n$ and $Q_{i,l}^n$, respectively.

As can be seen in (3) [38], when an operator engages in the bidding process, the bidding function is communicated to the bidding manager agent.

$$y_i^n = a_i^n \times Q_i^n + b_i^n, \quad a_i^n, b_i^n > 0. \tag{7}$$

At the bidding round n, y_i^n is the bidding price with the Q_i^n, whereas a_i^n and b_i^n are the bidding function price coefficients.

Q_i^n is essentially the operator's optimization goal and the operator's optimum power production for the electricity price P^n at the bidding round n. In other words, in bidding round $n+1$, the optimum bid function should theoretically pass the point (Q_i^n, P^n) and fulfill [39]

$$\begin{cases} Q_i^n = \dfrac{P^n - C_i^0}{2C_i^1}, \\ \\ P^n = a_i^{n+1} \times Q_i^n + b_i^{n+1}. \end{cases} \tag{8}$$

According to (4), the ideal price coefficients $a_{t,i}^{n+1}$ and $b_{t,i}^{n+1}$ are distributed in a downward spiral on the coordinate system. Based on the SGHSA, the bidding unit agent derives the bid function coefficients a_i^{n+1} and reports them to the bidding manager agent in this paper.

In this process, the generation constraint of the unit needs to be met. For the adjustable unit, the following formula can represent the electric energy generated by the dispatchable unit during the bidding of the n round. p_i^n is the output power of the dispatchable unit during the bidding of the n round. Δt is the time interval of the bidding round.

$$Q_i^n = \frac{p_i^{n-1} + p_i^n}{2} \Delta t. \tag{9}$$

Constraints are as follows.

3.1.1. Unit Output Constraints.

$$u_i p_i^{\min} \le p_i^n \le u_i p_i^{\max}, \tag{10}$$

$$u_i \in \{0, 1\}, \tag{11}$$

where $p_i^{\max}$ represents the upper and lower limits of the output power of the dispatchable unit and u_i is a binary variable. When u_i is 0, the unit is offline and shut down. When u_i is 1, the unit runs online.

3.1.2. Climbing Rate Constraint.

$$-R_g^D \Delta t \le p_i^n - p_i^{n-1} \le R_g^U \Delta t, \tag{12}$$

where R_g^D and R_g^U are the dispatchable unit's upward and downward climbing rates, respectively.

3.1.3. Constraints on Unit Start-Up and Shutdown Costs. Start and stop constraints are not listed here due to space limitations (refer to [37]).

Due to the substantial uncertainty of the output power of the random generator set (wind power and photovoltaic), the output power of the random generator set p_i^n does not exceed the available output power of the random generator set p_q.

$$0 \le p_i^n \le p_q. \tag{13}$$

3.2. The Clearing Process of Bidding Manager Agent. The bidding manager agent calculates the internal electricity price based on the supplied information and the load condition and distributes the power-generating amount to each bidding unit agent, as illustrated in (9).

$$\begin{cases} P^{n+1} = y_i^{n+1}\left(Q_i^{n+1}\right), \quad i = 1, 2, \ldots, l, \\ \\ D_{\text{load}} = \sum_{i=1}^{h} Q_i^{n+1}. \end{cases} \tag{14}$$

Suppose M is the smallest possible number of operators whose combined power generation has not been surpassed. Each operator's power production allocation and the internal energy price of the bidding round $n+1$ may be solved by the bidding management agent, as shown in the following equation:

$$P^{n+1} = \frac{\left[D^{\text{load}} + \sum_{i \in \mathbf{N}} P^n / b_i^{n+1} - \sum_{i \in \mathbf{M}} \left(P^n - C_i^0 / 2C_i^1\right) - \sum_{i \notin \mathbf{M}} Q_i^n\right]}{\sum_{i \in \mathbf{N}} 1 / b_i^{n+1}}, \tag{15}$$

where D_t^{load} represents the amount of demand that the VPP needs to meet.

Formula (10) can be simplified as follows:

$$P^{n+1} = P^n \times \left(1 - \frac{\sum_{i \in \mathbf{M}} 1/C_i^1}{2B^{n+1}}\right) + \frac{\sum_{i \in \mathbf{M}} C_i^0 / C_i^1 + 2D^{\text{load}'}}{2B^{n+1}}, \tag{16}$$

where $B_t^{n+1} = \sum_{i=1}^{N} 1/b_{t,i}^{n+1} D_t^{\text{load}'} = D_t^{\text{load}} - \sum_{i \notin M} Q_{t,i}^n D_t^{\text{load}'}$ represents the load left after subtracting the operator's power production that exceeds the limit.

Kong et al. [39] found that the bidding function's pricing coefficient is distributed on a straight line and not unique; therefore, the condition can be achieved by adequately defining the search range of bidding coefficients for all bidding agents, $0 < (\sum_{i \in \mathrm{M}} 1/c_i^1)/(2B_{n+1}) < 1$, and (17) depicts the power price convergence value P_{clear}:

$$P_{\text{clear}} = \frac{\sum_{i \in \mathbf{M}} C_i^0 / C_i^1 + 2D^{\text{load}'}}{\sum_{i \in \mathbf{M}} 1 / C_i^1}. \tag{17}$$

The VPP's decision-making process is depicted in Figure 3 by a flowchart. Using the SGHSA algorithm, the bidding unit agent finds the optimal bidding function $y_i^n = a_i^n \times Q_i^n + b_i^n$ and reports it to the bidding management agent, which contains the optimal bidding function coefficient and generation limit value $[(a_i^n, b_i^n), (Q_{\min}, Q_{\max})]$. The

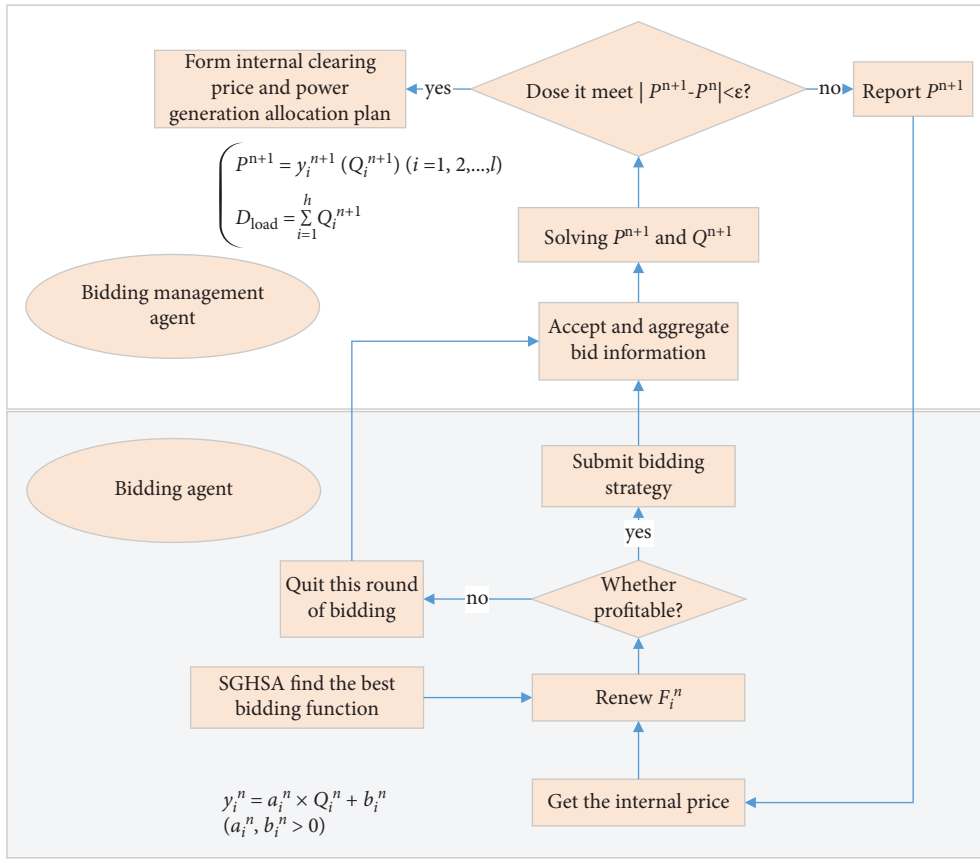

Figure 3: The flowchart of the decision-making process in the VPP.

bidding manager agent calculates and distributes to all bidding unit agents the new internal energy price P^{n+1} of the VPP and the power generation distribution scheme Q^{n+1} based on the bidding function supplied by the bidding unit agent and the current load demand. Each bidding agent modifies its bidding strategy based on the updated internal electricity price P^{n+1} and rereports it until price convergence in the VPP.

The SGHSA parameter's adaptive dynamic adjustment feature may solve the optimal bidding function for different bidding unit agents based on the VPP's internal electricity price, the generation cost, and the generation limit of other operators and maximize the advantages of operators.

4. DER Bidding Process Based on SGHSA

4.1. Definition of the Problem and Its Parameters. In this paper, the harmony vector of SGHSA is the optimal bidding function coefficient (a_i^n, b_i^n) of the bidding unit agent, and the evaluation criterion is the revenue function of the bidding unit agent. The corresponding relationship between the variables in this paper and the SGHSA parameters is shown in Table 1.

The parameters of SGHSA are shown in Table 2. The four main parameters of SGHSA are HMS, HMCR, PAR, and BW. The other three parameters are dynamically adjusted with the iterative search except for HMS, fixed after initialization.

Consider a normal distribution for the HMCR (PAR) with mean HMCR.m (here 0.98), PAR.m (here 0.9), and standard deviation 0.01 (0.05) [39]. The procedure begins with an HMCR and PAR value determined in accordance with the normal distribution. The HMCR and PAR values associated with the created harmony are then substituted for the poorest member of the HM. Then, a specified number of generations, called Learning Period (LP), HMCR.m and PAR.m, are recomputed by averaging all recorded HMCR and PAR values.The HMCR and PAR are recalculated and utilized in subsequent rounds using the new mean and existing standard deviation. Consequently, an appropriate HMCR and PAR value may be gradually learned for each unique situation by repeating this procedure. BW is adjusted dynamically with the change of iteration times Gen, as shown in the following equation:

$$BW(\text{Gen}) = \begin{cases} BW_{\max} - \dfrac{BW_{\max} - BW_{\min}}{T_{\max}} \cdot 2\text{Gen}; & \text{Gen} < \dfrac{T_{\max}}{2}, \\ BW_{\min}; & \text{Gen} \geq \dfrac{T_{\max}}{2}. \end{cases} \tag{18}$$

4.2. The Procedure of Solving the Coefficient of the Optimal Bidding Function Based on SGHSA. The fundamental harmonic search algorithm is divided into the following steps:

Table 1: The corresponding relationship between variables in this paper and SGHSA parameters.

No.	SGHSA	Music phenomenon	Variables in this paper
1	Decision variables	Music instruments	a_i^n, b_i^n
2	Range of variables	Range of notes	$LB(a_i^n)$, $UB(a_i^n)$; $LB(b_i^n)$, $UB(b_i^n)$
3	Solution vector	Harmony	$[a_i^n, b_i^n]$
4	Objective function	Standards of aesthetics	$F_i^n(a_i^n, b_i^n)$
5	Iteration	Practice	$T_{\max}$
6	Harmony memory	Experience	HM_i

Table 2: The SGHSA parameters and their abbreviation.

No.	SGHSA parameters	Abbreviation
1	Harmony memory size	HMS
2	Harmony memory considering the rate	HMCR
3	The mean of HMCR	HMCR.m
4	Pitch adjusting rate	PAR
5	The mean of PAR	PAR.m
6	Bandwidth	BW
7	The maximum of BW	$BW_{\max}$
8	The minimum of BW	$BW_{\min}$
9	Maximum iterations	$T_{\max}$
10	Learning period	LP
11	The change of iteration times	Gen
12	The current VPP internal electricity price	P^n
13	The operator i's profit in bidding round n	F_i^n
14	The electrical output during bidding round n	Q_i^n
15	The converted cost	C_i

(1) defining the problem and the parameter values; (2) initializing harmony memory (HM); (3) improvisation, generating a new harmony; (4) updating the harmony memory bank; and (5) checking whether the algorithm is terminated.

The core of the harmony search algorithm using the adaptive process is to improve HMCR, PAR, and BW and adjust direction. Major improvements include the following:

(1) *Adaptive Strategy of HMCR*. Since the HMCR of the standard harmony search algorithm is a fixed value, there is no concern about how to accelerate the convergence rate of harmony. Therefore, setting the HMCR to a dynamically changing value is necessary. At the initial optimization stage, a larger HMCR is used to find the optimal local value quickly. A smaller HMCR can increase the probability of random new solutions at the later optimization stage. The diversity of harmony effectively prevents falling into a locally optimal solution.

(2) *Adaptive Strategy of PAR*. Similarly, the PAR needs to be dynamically adjusted during the adaptive process to meet the difference between the early and late optimization stages. In contrast to HMCR, PARs need to be changed from small to large. In the early stage of algorithm optimization, minor PARs can quickly find the optimal local value. In contrast, larger PARs can increase the probability of being disturbed in the late stage of optimization and enrich the diversity of sounds.

(3) *Adaptive Strategy of BW*. In the standard harmony search algorithm, the BW of each set of harmony variables is the same. The same BW does not fit all harmonies. For the early and late stages of optimization, the length of BW needs to be adjusted to some extent. To this end, BW has been improved.

Based on the above discussion, the harmony search algorithm flow is obtained.

Step 1. Get the current electricity price.

Obtain the current VPP internal electricity price P^n and define the bidding unit agent i objective function using the equation provided below.

$$\max F_i^n = P^n \times Q_i^n - C_i, \tag{19}$$

where F_i^n is the operator i's profit in bidding round n, Q_i^n is the electrical output provided by the operator during round n of the bidding process, and C_i is the converted cost after accounting for the following elements and environmental protection measures.

Step 2. Calculate the relationship between the cost and generation.

Calculate agent i's maximum and minimum power generation limitations, and then enter the convertible cost coefficients C_i^1 and C_i^0, as well as the fixed cost coefficient C_i^{const}. For the DER operator i, determine the cost-to-generate connection between the two variables.

Step 3. Initialize the HM.

Set the upper and lower bounds $LB(a_i^n), UB(a_i^n), LB(b_i^n), UB(b_i^n)$ of the coefficients a_i^n and b_i^n as the initial values for the HM and compute the objective function's values. The HM has HMS (30 in this paper) vectors:

$$HM_i = \begin{pmatrix} X_i^1 \\ \vdots \\ X_i^J \\ \vdots \\ X_i^{HMS} \end{pmatrix} = \begin{pmatrix} a_i^{n1} & b_i^{n1} & F_i^{n1}\left(a_i^{n1}, b_i^{n1}\right) \\ \vdots & \vdots & \vdots \\ a_i^{nj} & b_i^{nj} & F_i^{nj}\left(a_i^{nj}, b_i^{nj}\right) \\ \vdots & \vdots & \vdots \\ a_i^{n30} & b_i^{n30} & F_i^{n30}\left(a_i^{n30}, b_i^{n30}\right) \end{pmatrix}, \tag{20}$$

where $a_i^{nj} = LB(a_i^n) + \text{rand}([0,1]) \times [UB(a_i^n) - LB(a_i^n)]b_i^{nj}$ is in the same way. The price coefficient range of bidding unit agent 1 in this paper is $a_1^n \in [1\times10^{-3}, 2\times10^{-3}]$, $b_1^n \in [0.10, 0.35]$ [11], so the HM_1 is as follows:

$$HM_1 = \begin{pmatrix} 1.71 \times 10^{-3} & 0.19 & 53.29 \\ \vdots & \vdots & \vdots \\ 1.43 \times 10^{-3} & 0.25 & 55.47 \\ \vdots & \vdots & \vdots \\ 1.25 \times 10^{-3} & 0.27 & 52.60 \end{pmatrix}. \quad (21)$$

Step 4. Modify new pricing coefficients.

Modify new pricing coefficients a_i^{new} and b_i^{new} in the methods described below. (1) Choose the best coefficients a_i^{best} andb_i^{best} of the HM. (2) Randomly generated withinthe value range of the bidding function coefficients a_i^n and$b_i^{n'}$ range of values. (3) Fine-tune the coefficients in the first two methods.

(i) Produce an HMCR value based on HMCR~N (0.98, 0.01) and generate a random number r_1 between [0, 1]. If $r_1 <$ HMCR, then take method (1) in step 4 to get the coefficients a_i^{new} and b_i^{new}; otherwise, take method (2) in step 4 to get the coefficients a_i^{new} and b_i^{new}.

(ii) Produce a PAR value based on PAR~N (0.9,0.05) and generate a random number r_2 between [0, 1]. If $r_2 <$ PAR, then fine-tune the optimal coefficients a_i^{best} and b_i^{best} in steps 4-(i) with the BW, which is related to the number of iterations. Otherwise, no adjustments.

a_1^{best} and b_1^{best} in the HM_1 are 1.43×10^{-3} and 0.25, and the randomly generated HMCR = 0.96, $r_1 = 0.67$, so $a_1^{\text{new}} = a_1^{\text{best}}$ and $b_1^{\text{new}} = b_1^{\text{best}}$ because $r_1 <$ HMCR. The randomly generated PRA = 0.75, $r_2 = 0.87$, so we do not do anything to a_1^{new} andb_1^{new} because $r_2 >$ PAR; then, $a_1^{\text{new}} = a_1^{\text{best}} = 1.43 \times 10^{-3}$ and $b_1^{\text{new}} = b_1^{\text{best}} = 0.25$.

The pseudo-code of the coefficients a_i^{new} and b_i^{new} is as follows.

```
HMCR~N (0.98, 0.01)
PAR~N (0.9, 0.05)
BW(Gen) = { BW_max
-(BW_max - BW_min/T_max) ·
2Gen; Gen < (T_max/2)BW_min; Gen ≥ (T_max/2)
for (j = 1 to 50) do
  if (rand[0, 1] < HMCR) then
    a_i^new = a_i^best
    b_i^new = b_i^best
    if (rand[0, 1] < PAR) then
      a_i^new = a_i^best ± BW × rand([0, 1])
      b_i^new = b_i^best ± BW × rand([0, 1])
    end if
  else
  a_i^new = LB(a_i^n) + rand([0, 1]) · [UB(a_i^n) − LB(a_i^n)]
  b_i^new = LB(b_i^n) + rand([0, 1]) · [UB(b_i^n) − LB(b_i^n)]
    end if
  end for
```

Step 5. Update the HM.

HMCR and PAR values should be recorded if the newly created coefficients a_i^{new} and b_i^{new} produce a higher profit $F_i^n(a_i^{\text{new}}, b_i^{\text{new}})$ than the lowest profit $F_i^n(a_i^{\text{new}}, b_i^{\text{new}})$ in the existing HM.

The profit (55.47) corresponded by the newly generated harmony in step 4 is more than the worst profit(52.6) in the [The newly generated harmony$a_1^{\text{new}\ -3} b_1^{\text{new}}$ in Step 4 corresponding profit$F_i^n(1.43 \times 10^{-3}, 0.25)$ (55.47) is more than the worst profit $F_i^n(1.25 \times 10^{-3}, 0.27)$(52.6) in the] HM_1. Therefore, the worst harmony is substituted with the new connection (a_1^{new}, b_1^{new}). Furthermore, memorize the HMCR and PAR values. The updated HM_1 is as follows:

$$HM_1 = \begin{pmatrix} 1.71 \times 10^{-3} & 0.19 & 53.29 \\ \vdots & \vdots & \vdots \\ 1.43 \times 10^{-3} & 0.25 & 55.47 \\ \vdots & \vdots & \vdots \\ 1.43 \times 10^{-3} & 0.25 & 55.47 \end{pmatrix}. \quad (22)$$

Step 6. Recompute HMCR.m and PAR.m.

Repeat steps 4 and 5. If Gen = LP, recompute HMCR.m and PAR.m based on memorized values of ones.

When Gen = LP = 50, based on the previously recorded HMCR (PAR) value, it can be recalculated that HMCR.m = 0.95, PAR.m = 0.87, so HMCR~N (0.95,0.01) and PAR~N (0.87,0.05) were used for the subsequent iterative search.

Step 7. Determine whether to terminate.

If Gen = $T_{\max}$, output the optimal bid function coefficients a_i^n and b_i^n.

After the above operation steps, the final optimal bidding function coefficient of agent 1 is obtained: a_1^n and b_1^n are equal to 1.47×10^{-3} and 0.24, respectively.

The flowchart for explaining the optimal bidding based on SGHSA is shown in Figure 4.

5. Case Studies

Verifying the SGHSA algorithm's efficacy in bidding function search is based on the creation of the VPP system in [11]. As indicated in Table 3, the following are the DER's costs and power limitations. There are three DER operators in the VPP. Each of the three operators has one or more of the following components: WT1, PV1, MT1, WT2, MT2, PV2, and MT3. Set the value of δ_{WT} to 0.2. Set the value of δ_{PV} to 0.1, with a price convergence precision of 0.01. Table 4 lists the SGHSA and HS parameters used in this study.

To test the effectiveness of SGHSA, this case uses three classical test functions as the benchmark functions. It makes a comparative analysis of the optimization results of SGHSA and HS algorithms under the condition that the

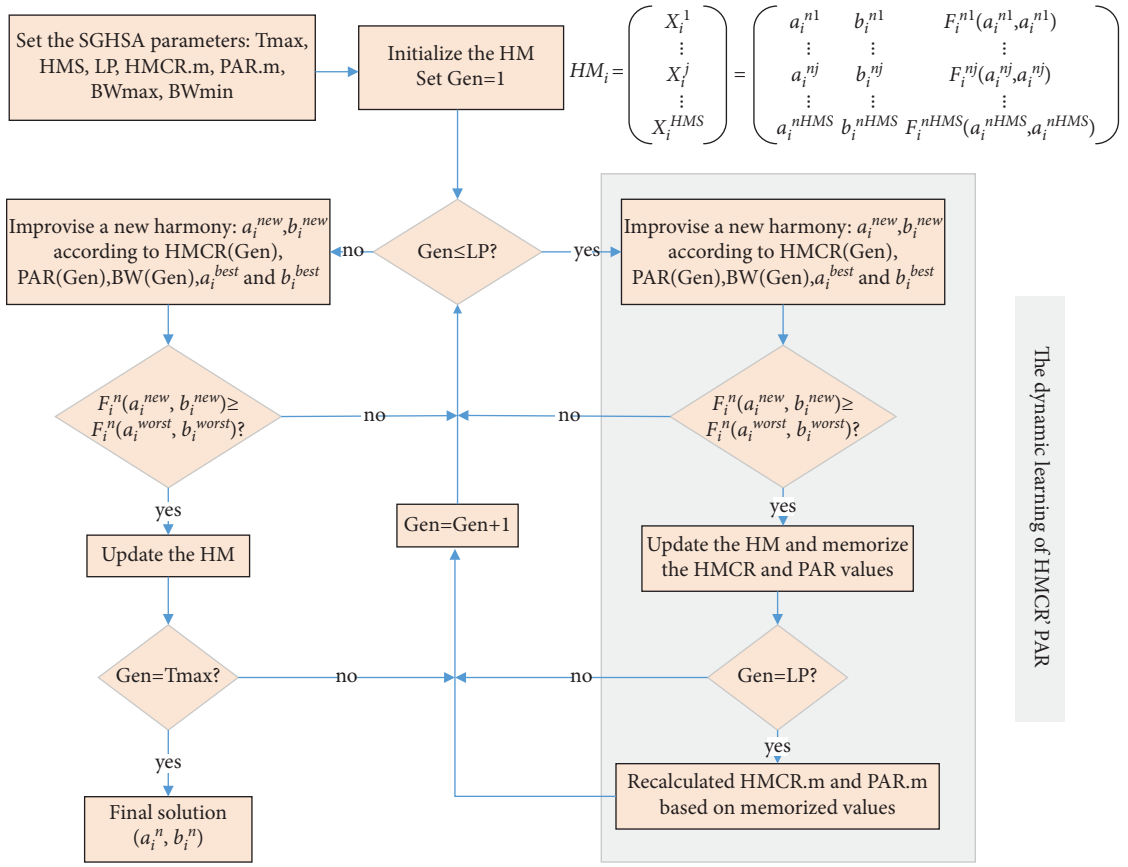

Figure 4: The flowchart for explaining the optimal bidding function based on SGHSA.

Table 3: Costs of factories and power constraints of the DERs (Table 3 is reproduced from [10]).

No.	DG	Cost coefficient/ ¥ $C^1Q^2 + C^0Q + C^{const}$			Q_{min} (kW)	Q_{max} (kW)
		C^1	C^0	C^{const}		
Operator 1	WT1	0	0.02	0	0	200
	PV1	0	−0.01	0	0	150
	MT1	3.33×10^{-3}	0.050	5	5	180
Operator 2	WT2	0	0.02	0	0	200
	MT2	3.33×10^{-3}	0.050	10	10	120
Operator 3	PV2	0	0.01	0	0	240
	MT3	1.67×10^{-3}	0.067	60	60	180

optimization operations of the three test functions are run separately 50 times. The concerned indexes are the objective function value of iteration completion, the average function value, and the standard deviation of the function value of the results of 50 runs. F_1–F_3 were compared after 5000 iterations in 10 and 30 dimensions, respectively (Table5).

To better understand the test results, Table 6 records the test comparison results 50 times from a numerical perspective, where Dim represents the dimension, and MEAN represents the average value of the optimal harmony function, which is used to reflect the convergence accuracy of the algorithm. STDV represents the standard deviation of the optimal harmony function value, which is used to remember the algorithm's stability.

Table 4: The parameters of SGHSA and HS.

No.	HS		SGHSA	
	Parameter	Value	Parameter	Value
1	HMS	30	HMS	30
2	HMCR	0.85	HMCR.m	0.98
3	PAR	0.8	PAR.m	0.9
4	BW_{max}	0.9	BW_{max}	0.9
5	BW_{min}	0.4	BW_{min}	0.4
6	T_{max}	100	T_{max}	100
7	—	—	LP	50

It can be seen from the table that SGHSA has good global optimization and adaptive ability in most cases. For example, for functions F_1 and F_2, MEAN and STDV are smaller than the HS algorithm when the dimension is 10 and 30.

To assess the efficacy and rationale of SGHSA, SGHSA was compared with HS. The number of previous iterations in SGHSA is the dynamic learning process of parameters HMCR and PAR. For the convenience of comparison with HS, the active learning process is not presented in the figure, and only the simulation process after the completion of dynamic learning is captured. When the internal electricity price issued by the bidding unit agent is 0.49 ¥ , the dynamic simulation process of the quotation coefficient of operator 1 is shown in Figures 5 and 6. The operator's optimal price coefficient converges rapidly in the 25th iteration based on

Table 5: The expressions and characteristics of 3 classical test functions.

No.	The function name	Functional expression	The search space	Minimum function value
F_1	Sphere	$f(x) = \sum_{i=1}^{n} x_i^2$	$[-5.12, 5.12]$	0
F_2	Rosenbrock	$f(x) = \sum_{i=1}^{n-1} [100(x_{i+1} - x_i^2) + (x_i - 1)^2]$	$[-30, 30]$	0
F_3	Ackley	$f(x) = -20\exp(-0.2\sqrt{(1/n)\sum_{i=1}^{n} x_i^2}) - \exp((1/n)\sum_{i=1}^{n}\cos(2\pi x_i)) + 20 + \exp(1)$	$[-32, 32]$	0

Table 6: Comparison of the experimental results.

No.	Dim	HS		SGHSA	
		MEAN	STDV	MEAN	STDV
F_1	10	4.00×10^{-100}	1.70×10^{-101}	0	0
	30	2.55×10^{-34}	2.49×10^{-35}	4.80×10^{-146}	1.78×10^{-146}
F_2	10	8.14×10^{0}	5.25×10^{-2}	1.44×10^{-4}	6.79×10^{-6}
	30	2.82×10^{1}	7.26×10^{-5}	7.19×10^{-6}	1.79×10^{-7}
F_3	10	2.36×10^{-1}	8.32×10^{-17}	2.36×10^{-1}	8.32×10^{-17}
	30	8.62×10^{-2}	0	8.62×10^{-2}	0

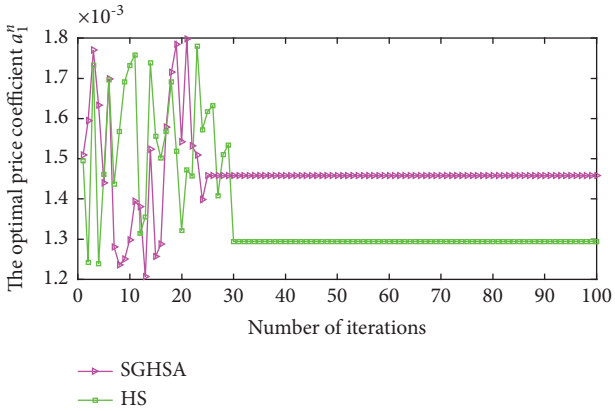

Figure 5: Dynamic simulation process of optimal price coefficient a_1^n of operator 1.

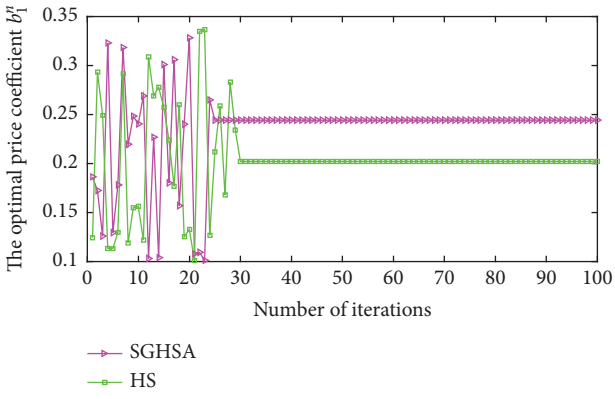

Figure 6: Dynamic simulation process of optimal price coefficient b_1^n of operator 1 (Figures 5 and 6 are reproduced from [10]).

SGHSA, while based on the HS they converge in the 30th iteration.

Figure 7 provides the VPP internal price convergence process. The internal electricity price converges rapidly to ¥0.424 at the 14th iteration, between the main grid purchase and sale price (¥0.37 and ¥0.66). The bidding and trading system can boost the revenue of operators and the

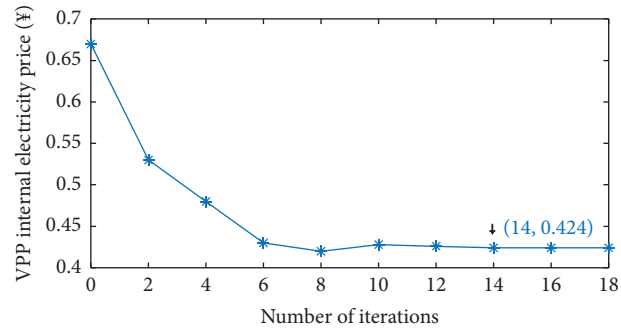

Figure 7: The VPP internal price convergence process.

motivation of the VPPs to engage in peak adjustment of the main grid. Meanwhile, the load users in the VPP can reduce the power consumption cost. For the main grid, the advantages of the VPP can be fully utilized to relieve the power supply pressure of the power grid.

Quadratic programming based on the equilibrium method (QPEM) [40, 41] is used to allocate the power generation of the operator and then compared with the method proposed in this paper. When using the QPEM method, The VPP dispatching center conducts electricity settlement with the operator based on the power purchase price of the enormous power grid. It sells electricity to users based on the power sale price of the power grid. Table 7 displays the distribution, profit, and internal electricity price for each operator based on SGHSA, HS, and QPEM, respectively

After the bidding strategy is adopted to distribute operators' power generation, each operator's power generation profit is higher than that of QPEM, mainly because the electricity generation obtained by operators through the method proposed in this section is higher than the QPEM. The internal electricity price of VPP is greater than or equal to the electricity purchase price of the grid in each period. Since the QPEM method sells electricity to users according to the electricity selling price of the grid, the proposed method sells electricity according to the internal cost of VPP, which is less than or equal to the electricity selling price of the grid in each period. Hence, the electricity price of the users calculated by the proposed method is lower than that of the QPEM.

Virtual power plant bidding functions are directly influenced by load users who do not engage in the bidding process because of a restricted number of DER operators. With an optimum bidding function based on the SGHSA, the bidding unit agent may increase operator profit while also maximizing their interests.

Figure 8 shows operator 1's whole-day power generation and DER scheduling results. It can be seen from the figure

Table 7: Comparison of the effects of SGHSA and HS.

No.	Power generation (kWh)/profit (¥)			Internal electricity price (¥)
	Operator 1	Operator 2	Operator 3	
SGHSA	138.15/56.53	140.56/54.29	189.75/74.28	0.424
HS	144.39/53.21	115.20/43.04	112.84/41.05	0.417
QPEM	139.42/54.22	120.20/49.82	133.62/60.05	0.419

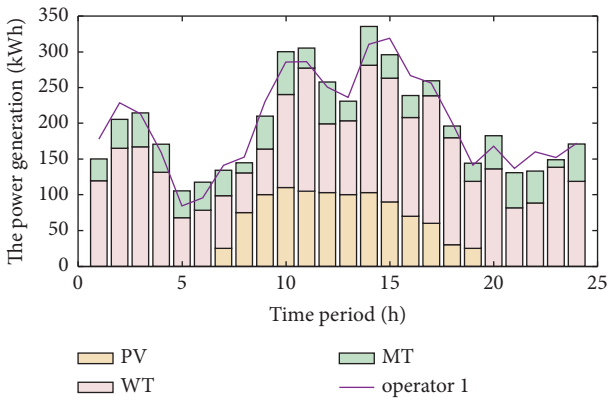

Figure 8: The power generation of operator 1 and its DER dispatching results.

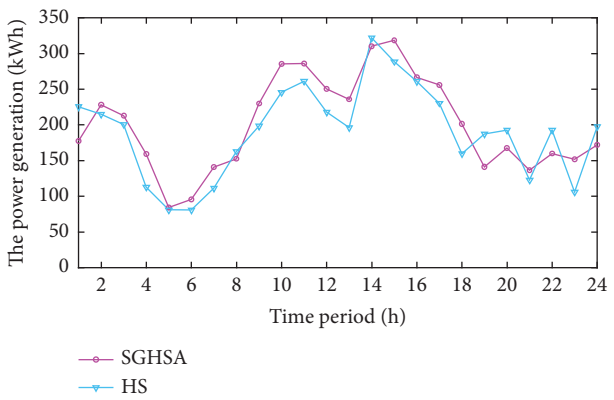

Figure 9: The power generation of operator 1 based on SGHSA and HS, respectively.

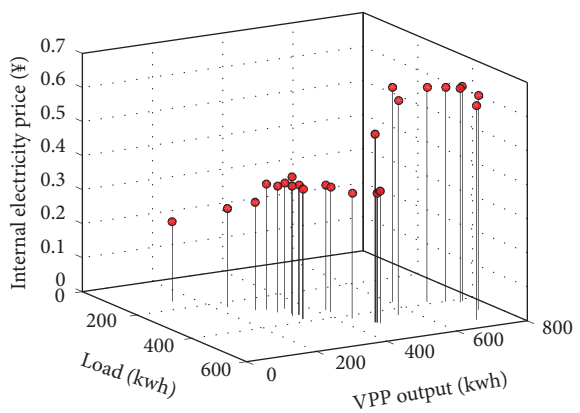

Figure 10: Schematic diagram of a variation of internal electricity price, load, and the VPP output.

that the operator's DER does not generate power based on the bid-winning power, which may take demand response and charge and discharge of energy storage into consideration, and the VPP makes secondary adjustments to its plan. In addition, when the power load is low, the wind abandoning phenomenon will occur in the power system with new energy access. Due to the limitation of the power transmission and the node voltage, it is impossible to absorb all the new energy during the peak load, and hence, different degrees of abandonment exist. This scheduling mode fully respects the autonomy of each operator, effectively alleviates the phenomenon of abandoning wind and light, and improves the energy utilization rate while increasing the operator's income.

Figure 9 shows the power generation of operator 1 based on SGHSA and HS, and the bid-winning electric quantity based on SGHSA is higher than HS in more than two-thirds of a day. Generally, the operator's bid-winning power based on SGHSA is higher than that of HS. The parameter adaptation of SGHSA can gradually learn the appropriate HMCR (PAR) to adapt to specific problems and stages of the search and maximize the operator's profit, proving the superiority of SGHSA in the bidding strategy search for the virtual power plant.

Figure 10 shows the relationship between the VPP's internal electricity price, total power generation, and load. As can be seen from the overall trend in the figure, when the load and the VPP's power generation are large, the internal electricity price of the VPP is relatively high. When the load and the VPP's power generation are small, the internal electricity price of the VPP is low. This indicates that the internal price of the VPP conforms to the economic law that increases with demand and cost and can be seen as a reflection of the connection between supply and demand.

6. Conclusion

This paper proposes an optimal bidding method for multi-operator VPP based on SGHSA. Aiming at the inherent shortcomings of the traditional harmony algorithms, such as slow convergence speed and low search accuracy, a new adaptive global optimal harmony search algorithm is proposed by improving the improvisation stage of the HS algorithm. The simulation results show that the proposed SGHSA has good global optimization and adaptive ability, and the algorithm has good robustness. Using this algorithm in the VPP bidding and trading can improve the operators' bidding ability, provide a friendly interaction mode between the VPP and the main power grid through price

information, and optimize the allocation of energy resources. At the same time, it can represent the supply and demand connections within the virtual power plant, increasing the profits generated by the generator for the operator. In conclusion, this method can effectively make the operation of the VPP more economical and flexible and can improve the enthusiasm of the DER operators to participate in the VPP.

To obtain the results that are applicable for the long term, it is insufficient to analyze the load data of a specific day. The scheduling problem of the operator's internal DER after the bidding is not discussed in this paper. For future work, considering the uncertainty of the DER output, we will further study how the operators conduct the DER scheduling to reduce the loss caused by bidding deviation.

Data Availability

The constraint and parameter data used to support the findings of this study are included within the article.

Conflicts of Interest

The authors declare that they have no conflicts of interest.

Acknowledgments

This study was supported by the Science and Technology Project of State Grid Tianjin Electric Power Company (Key Technologies Research on Interaction Characteristics of Source-Grid-Load and Power Quality Management based on Distribution Internet of Things).

References

[1] X. Kong, J. Xiao, C. Wang, K. Cui, Q. Jin, and D. Kong, "Bi-level multi-time scale scheduling method based on bidding for multi-operator virtual power plant," *Applied Energy*, vol. 249, pp. 178–189, 2019.

[2] B. Li, H. Yihao, and B. Qi, "Key information communication technologies supporting virtual power plant interaction," *Power System Technology*, vol. 46, no. 5, pp. 1761–1770, 2022.

[3] W. Song, J. Wang, and H. Zhao, "Research on multi-stage bidding strategy of virtual power plant considering demand response market," *Power System Protection and Control*, vol. 45, no. 19, pp. 35–45, 2017.

[4] L. Zhao, X. Wang, and Y. Ding, "Optimal dispatch of multi-energy virtual power plant considering time-of-use electricity price and CSP plant," *Electric Power Construction*, vol. 43, no. 4, pp. 119–129, 2022.

[5] C. Hou, H. Liang, and D. Zhao, "Game theory based optimization allocation of generators in virtual power plant," *Modern Electric Power*, vol. 37, no. 4, pp. 376–384, 2020.

[6] B. Hong, Q. Li, and Y. He, "Applications and prospect of virtual power plant in distributed photovoltaic generation application demonstration area," *Electric Power Construction*, vol. 38, no. 09, pp. 32–37, 2017.

[7] F. Xu, Y. He, and J. Li, "Review of research on commercial mechanism for virtual power plant considering demand response," *Power Demand Side Management*, vol. 21, no. 03, pp. 2–6, 2019.

[8] X. Li, W. Wang, and H. Wang, "Bi-Level and multi-objective robust optimal dispatching of AC/DC hybrid microgrid with virtual power plant participation," *High Voltage Engineering*, vol. 46, no. 7, pp. 2350–2361, 2022.

[9] X. Kong, D. Liu, J. Xiao, and C. Wang, "A multi-agent optimal bidding strategy in microgrids based on artificial immune system," *Energy*, vol. 189, Article ID 116154, 2019.

[10] S. Zhang, X. Kong, and Y. Shen, "Optimal economic dispatch of virtual power plant based on bidding," in *Proceedings of the 2020 23rd International Conference on Electrical Machines and Systems*, pp. 467–471, November 2020, Hamamatsu, Japan.

[11] X. Kong, D. Kong, J. Yao, L. Bai, and J. Xiao, "Online pricing of demand response based on long short-term memory and reinforcement learning," *Applied Energy*, vol. 271, Article ID 114945, 2020.

[12] E. G. Kardakos, C. K. Simoglou, and A. G. Bakirtzis, "Optimal offering strategy of a virtual power plant: astochastic bi-level approach," *IEEE Transactions on Smart Grid*, vol. 7, no. 2, pp. 794–806, 2016.

[13] M. Shafiekhani, A. Badri, M. Shafie-khah, and J. P. Catalao, "Strategic bidding of virtual power plant in energy markets: a bi-level multi-objective approach," *International Journal of Electrical Power & Energy Systems*, vol. 113, pp. 208–219, 2019.

[14] A. Shahmohammadi, R. Sioshansi, A. J. Conejo, and S. Afsharnia, "Market equilibria and interactions between strategic generation, wind, and storage," *Applied Energy*, vol. 220, pp. 876–892, 2018.

[15] S. Ahmad, M. M. Alhaisoni, M. Naeem, A. Ahmad, and M. Altaf, "Joint energy management and energy trading in residential microgrid system," *IEEE Access*, vol. 8, pp. 123334–123346, 2020.

[16] S. Ahmad, M. Naeem, and A. Ahmad, "Unified optimization model for energy management in sustainable smart power systems," *International Transactions on Electrical Energy Systems*, vol. 30, no. 4, Article ID e12144, 2020.

[17] H. Ahmad, A. Ahmad, and S. Ahmad, "Efficient energy management in a microgrid," in *Proceedings of the International Conference on Power Generation Systems and Renewable Energy Technologies (PGSRET)*, pp. 1–5, USA, 2018.

[18] R. Yaqub, S. Ahmad, A. Ahmad, and M. Amin, "Smart energy-consumption management system considering consumers' spending goals (SEMS-CCSG)," *International Transactions on Electrical Energy Systems*, vol. 26, no. 7, pp. 1570–1584, 2016.

[19] S. Ahmad, M. Naeem, and A. Ahmad, "Low complexity approach for energy management in residential buildings," *International Transactions on Electrical Energy Systems*, vol. 29, no. 1, Article ID e2680, 2019.

[20] M. Shivaie and M. T. Ameli, "An environmental/techno-economic approach for bidding strategy in security-constrained electricity markets by a bi-level harmony search algorithm," *Renewable Energy*, vol. 83, pp. 881–896, 2015.

[21] Y. Wang, Z. Guo, and Y. Wang, "Enhanced harmony search with dual strategies and adaptive parameters," *Soft Computing*, vol. 21, no. 15, pp. 4431–4445, 2017.

[22] Z. Guo, H. Yang, S. Wang, C. Zhou, and X. Liu, "Adaptive harmony search with best-based search strategy," *Soft Computing*, vol. 22, no. 4, pp. 1335–1349, 2018.

[23] J. Yi, X. Li, C.-H. Chu, and L. Gao, "Parallel chaotic local search enhanced harmony search algorithm for engineering

design optimization," *Journal of Intelligent Manufacturing*, vol. 30, no. 1, pp. 405–428, 2019.

[24] Y. Xue, J. Jiang, B. Zhao, and T. Ma, "A self-adaptive artificial bee colony algorithm based on global best for global optimization," *Soft Computing*, vol. 22, no. 9, pp. 2935–2952, 2018.

[25] M. Shivaie, M. T. Ameli, M. S. Sepasian, P. D. Weinsier, and V. Vahidinasab, "A multistage framework for reliability-based distribution expansion planning considering distributed generations by a self-adaptive global-based harmony search algorithm," *Reliability Engineering & System Safety*, vol. 139, pp. 68–81, 2015.

[26] M.-Y. Cheng, D. Prayogo, Yu-W. Wu, and M. M. Lukito, "A hybrid harmony search algorithm for discrete sizing optimization of truss structure," *Automation in Construction*, vol. 69, pp. 21–33, 2016.

[27] F. Schaedler de Almeida, "Optimization of laminated composite structures using harmony search algorithm," *Composite Structures*, vol. 221, Article ID 110852, 2019.

[28] J. Yi, L. Gao, X. Li, C. A. Shoemaker, and C. Lu, "An on-line variable-fidelity surrogate-assisted harmony search algorithm with multi-level screening strategy for expensive engineering design optimization," *Knowledge-Based Systems*, vol. 170, pp. 1–19, 2019.

[29] S. Li, D. Zhang, Z. Shao, and H. Tang, "Information feedback self-adaptive harmony search algorithm for the bovine cortical bone vibration-assisted drilling optimization," *Measurement*, vol. 149, Article ID 107020, 2020.

[30] Z. A. Shaffiei, Z. A. Abas, N. M. Yunos, A. S. S. S. Amir Hamzah, Z. Z. Abidin, and C. K. Eng, "Constrained self-adaptive harmony search algorithm with 2-opt swapping for driver scheduling problem of university shuttle bus," *Arabian Journal for Science and Engineering*, vol. 44, no. 4, pp. 3681–3698, 2019.

[31] R. Zhang, S. Aziz, M. U. Farooq et al., "A wind energy supplier bidding strategy using combined EGA-inspired HPSOIFA optimizer and deep learning predictor," *Energies*, vol. 14, no. 11, p. 3059, 2021.

[32] L. Xiong, P. Li, Z. Wang, and J. Wang, "Multi-agent based multi objective renewable energy management for diversified community power consumers," *Applied Energy*, vol. 259, Article ID 114140, 2020.

[33] X. Ye, J. Le, Y. Liu, W. Zhou, and K. Liu, "A coordinated consistency voltage stability control method of active distribution grid," *Journal of Modern Power Systems and Clean Energy*, vol. 6, no. 1, pp. 85–94, 2018.

[34] Q. Sun, R. Han, H. Zhang, J. Zhou, and J. M. Guerrero, "A multiagent-based consensus algorithm for distributed coordinated control of distributed generators in the energy internet," *IEEE Transactions on Smart Grid*, vol. 6, no. 6, pp. 3006–3019, 2015.

[35] C. Dou, X. Jia, and H. Li, "Multi-agent-system-based market bidding strategy for distributed generation in microgrid," *Power System Technology*, vol. 40, no. 2, pp. 579–586, 2016.

[36] S. Liu, A. Qian, and J. Zheng, "Bi-Level coordination mechanism and operation strategy of multi-time scale multiple virtual power plants," *Proceedings of the CSEE*, vol. 38, no. 3, pp. 753–761, 2018.

[37] H. Wang, J. Wang, and C. Wang, "Risk-constrained energy management modeling of virtual power plant," *Proceedings of the CSEE*, vol. 37, no. 20, pp. 942–5950, 2017.

[38] Q. He and A. Qian, "Bidding strategy of electricity market including virtual power plant considering demand response under retail power market deregulation," *Electric Power Construction*, vol. 40, no. 2, pp. 1–10, 2019.

[39] X. Kong, Y. Ma, and L. Ye, "Remote estimation method for measurement error of smart meter based on limited memory recursive least squares algorithm," *Proceedings of the CSEE*, vol. 40, no. 7, pp. 2142–2151, 2020.

[40] L. Zhang, C. Xu, and Y. He, "Day-ahead market clearing model compatible with medium-and long-term physical contracts," *Automation of Electric Power Systems*, vol. 45, no. 6, pp. 16–25, 2021.

[41] A. Qi, J. Wang, and G. Li, "Scheme and method for market participation of virtual power plant based on equilibrium theory," *Electric Power Construction*, vol. 41, no. 6, pp. 1–8, 2020.